Journal of Controlled Release 390 (2026) 114520

Contents lists available at ScienceDirect

Journal of Controlled Release

journal homepage: www.elsevier.com/locate/jconrel

mRNA based in vivo MG1113 antibody production as a potential therapeutic approach for hemophilia

Miyoung Oh [a,b], Yujeong Jeong [a], Hyein Jung [a], Yongjoo Byeon [e], Heechun Kwak [c], Songseop Kim [d], Wonhyo Seo [a], Jaesung Jung [b], Hyukjin Lee [a,e,*]

[a] College of Pharmacy, Graduate School of Pharmaceutical Sciences, Ewha Womans University, Seoul 03760, Republic of Korea
[b] mRNA Research Team, GC Biopharma, 93 Ihyeon-ro 30-beongil, Giheung-gu, Yongin-si, Gyeonggi-do 16924, Republic of Korea
[c] Discovery Team, GC Biopharma, 93 Ihyeon-ro 30-beongil, Giheung-gu, Yongin-si, Gyeonggi-do 16924, Republic of Korea
[d] Non-Clinical Research Team, GC Biopharma, 93 Ihyeon-ro 30-beongil, Giheung-gu, Yongin-si, Gyeonggi-do 16924, Republic of Korea
[e] College of Pharmacy, Seoul National University, Seoul 08826, Republic of Korea

ARTICLE INFO

Keywords:
mRNA-based therapeutic antibody
Lipid nanoparticle
TFPI
mRNA-MG1113
Hemophilia

ABSTRACT

Hemophilia is a genetic bleeding disorder caused by deficiencies in coagulation factor VIII or IX. Although current therapies—including factor replacement, bispecific antibodies, and gene therapy—have improved disease management, they are limited by short half-lives, immunogenicity, complex manufacturing processes, and the need for repeated administration. Here, we report a lipid nanoparticle (LNP)- encapsulated messenger RNA (mRNA) encoding MG1113, a humanized monoclonal antibody that targets tissue factor pathway inhibitor (TFPI), enabling sustained in vivo antibody production as a factor-unrelated therapeutic strategy. The mRNA was optimized with a tailored signal peptide, regulatory UTRs, uridine depletion, and N1-methyl-pseudouridine incorporation to enhance the efficiency and stability of its translation. Systemic administration of the MG1113 mRNA-LNPs to mice and rabbits led to robust and durable antibody expression, efficient plasma TFPI suppression, and extended pharmacodynamic effects compared with direct administration of the recombinant MG1113 protein. This study explores an mRNA-LNP platform for antibody delivery in hemophilia, offering the potential for prolonged pharmacological activity, simplified manufacturing, and flexible therapeutic application. Taken together, our findings suggest that mRNA LNP systems could advance next-generation antibody-based treatment strategies for bleeding disorders and potentially other diseases.

1. Introduction

Hemophilia is a rare, inherited bleeding disorder caused by deficiencies in coagulation factor VIII (hemophilia A) or factor IX (hemophilia B), leading to impaired thrombin generation and an elevated risk of spontaneous and prolonged bleeding episodes [1]. Conventionally, this condition is managed by intravenous infusion of the missing clotting factor, which can effectively prevent or control bleeding. However, this approach is associated with limitations including a short half-life, the need for frequent dosing, and the risk of developing neutralizing antibodies that compromise therapeutic efficacy [2–4]. These challenges not only lower patient adherence but also significantly diminish quality of life.

Recent advances in factor-unrelated therapies, such as bispecific antibodies, have enabled subcutaneous administration and improved efficacy in patients with inhibitory antibodies [5,6]. However, these agents are associated with risks of immune-mediated adverse effects and thrombosis, as well as highly complex processes for producing them and the need for their continuous administration. Similarly, gene therapies hold promise for long-term correction of coagulation factor deficiency, but face substantial hurdles, including host immune responses to viral vectors, uncertain durability, hepatotoxicity, and high cost [7,8]. Collectively, these limitations highlight the need for alternative strategies that offer durable efficacy, reduced immunogenicity, and improved patient convenience [4,9–11].

Among emerging alternatives, therapeutic modulation of endogenous anticoagulant pathways has shown considerable promise. Tissue factor pathway inhibitor (TFPI), a critical regulator of the extrinsic coagulation cascade, functions by inhibiting the TF/FVIIa/FXa complex and prothrombinase activity [12]. The inhibition of TFPI can restore

* Corresponding author at: College of Pharmacy, Seoul National University, 1 Gwanak-ro, Gwanak-gu, Seoul 08826, Republic of Korea.
E-mail address: hyukjin@snu.ac.kr (H. Lee).

https://doi.org/10.1016/j.jconrel.2025.114520
Received 4 December 2025; Accepted 6 December 2025
Available online 7 December 2025
0168-3659/© 2025 The Authors. Published by Elsevier B.V. This is an open access article under the CC BY license (http://creativecommons.org/licenses/by/4.0/).

thrombin generation and improve hemostasis in hemophilia A and B, regardless of the presence of factor inhibitors. Several anti-TFPI antibodies, including marstacimab and concizumab, have recently advanced to regulatory approval, confirming TFPI as a clinically actionable target [13,14]. Nevertheless, conventional protein-based delivery of these antibodies remains limited by production bottlenecks, stability concerns, and the need for repeated dosing [15–20]. The emergence of in vivo-translatable mRNA technology offers a new therapeutic paradigm. Synthetic mRNA encapsulated in lipid nanoparticles (mRNA-LNPs) enables transient, controlled, and scalable production of therapeutic proteins directly within the body, bypassing many limitations of recombinant protein therapies [21–25]. This approach combines the high specificity of antibody-based targeting with the pharmacokinetic and manufacturing advantages of mRNA delivery platforms.

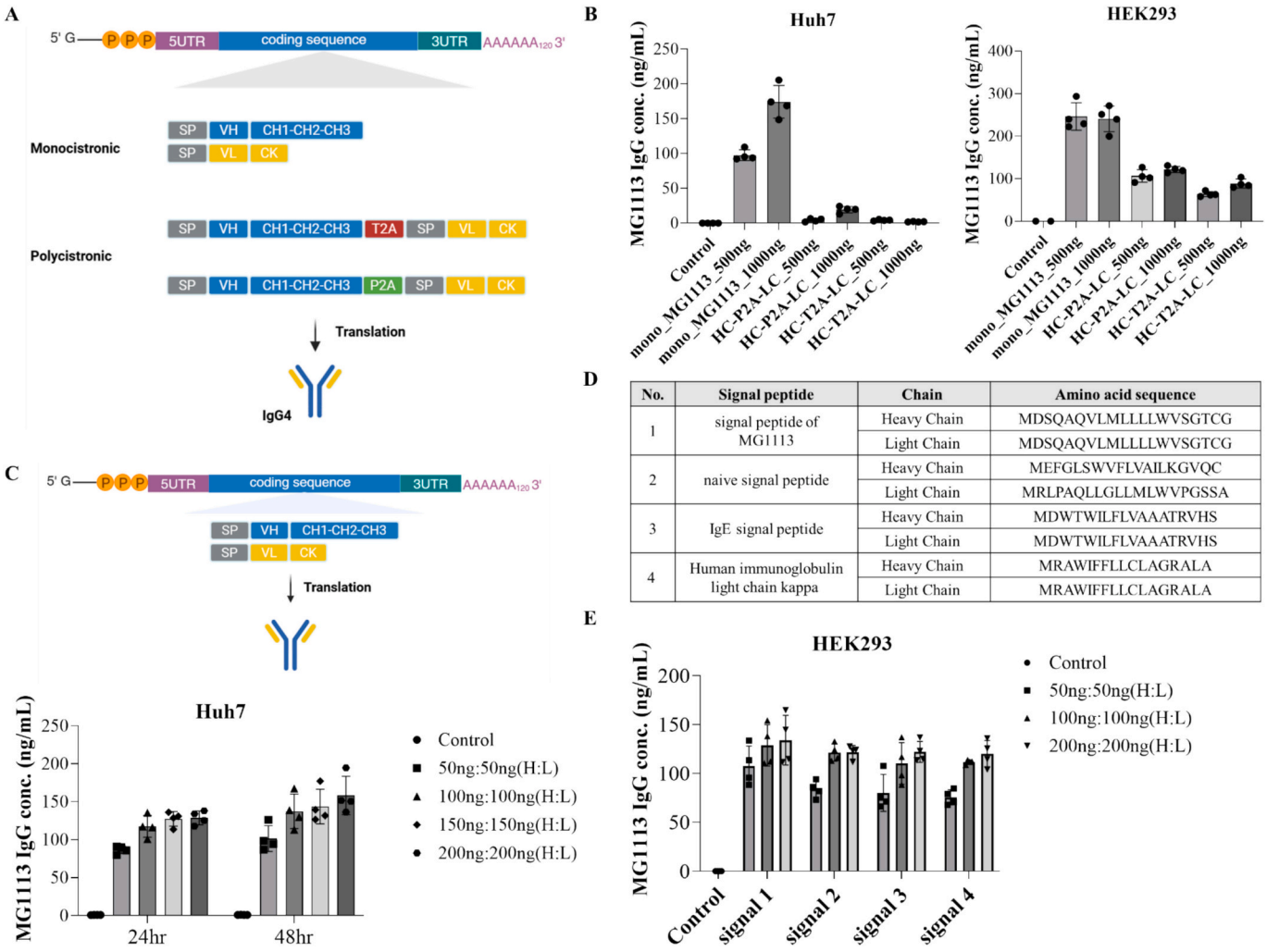
MG1113 is a fully human monoclonal antibody that targets TFPI for the prophylactic treatment of hemophilia A and B [26,27]. Although its recombinant form has demonstrated efficacy in preclinical and early clinical studies, its production and administration are constrained by challenges associated with the delivery of conventional biotherapeutics. Here, we report the development and in vivo validation of an optimized mRNA-LNP system encoding MG1113 as a next-generation factor-unrelated therapy for hemophilia. To maximize expression and therapeutic activity, the MG1113 mRNA was engineered with an optimized signal peptide and codon usage, regulatory UTRs, and nucleoside modifications (including uridine depletion and N1-methyl-pseudouridine incorporation). Liver-targeted LNPs were employed for systemic delivery, enabling robust antibody production in vivo. Pharmacokinetic and pharmacodynamic studies in both murine and rabbit models demonstrated sustained MG1113 expression, effective TFPI suppression, and prolonged therapeutic activity compared with the direct administration of the recombinant protein.

Here, we investigated an mRNA-LNP platform that enables sustained in vivo MG1113 expression as a scalable therapy for hemophilia. This approach may overcome limitations of recombinant antibodies and support rapid development of therapies for bleeding disorders.

2. Results

2.1. Construct screening for mRNA-encoded MG1113 IgG4 expression in vitro

As shown in Fig. 1A, the HC- and LC-encoding mRNA molecules



No.	Signal peptide	Chain	Amino acid sequence
1	signal peptide of MG1113	Heavy Chain	MDSQAQVLMLLLLWVSGTCG
		Light Chain	MDSQAQVLMLLLLWVSGTCG
2	naive signal peptide	Heavy Chain	MEFGLSWVFLVAILKGVQC
		Light Chain	MRLPAQLLGLLMLWVPGSSA
3	IgE signal peptide	Heavy Chain	MDWTWILFLVAAATRVHS
		Light Chain	MDWTWILFLVAAATRVHS
4	Human immunoglobulin light chain kappa	Heavy Chain	MRAWIFFLLCLAGRALA
		Light Chain	MRAWIFFLLCLAGRALA

Fig. 1. Construct screening for mRNA-encoded MG1113 IgG4 expression in vitro. (A) Schematic of monocistronic and polycistronic mRNA designs. Monocistronic constructs encode HC and LC on separate mRNAs, each with its own signal peptide (SP), while polycistronic constructs co-express HC and LC on a single mRNA separated by T2A or P2A self-cleaving peptides. (B) MG1113 antibody levels in HEK293 and Huh7 cell culture supernatants 24 h post-transfection, quantified by ELISA. (C) Schematic of monocistronic mRNA constructs encoding separate HC and LC chains (top), and MG1113 antibody levels in Huh7 cell supernatants at 24 and 48 h post-transfection (bottom). (D) Amino acid sequences of signal peptides tested for the HC and LC of MG1113. (E) MG1113 antibody production in HEK293 cells 24 h post-transfection with mRNAs containing different signal peptides. Data are presented as mean ± SD ($n = 4$).

consist of a 5′ cap structure, 5′ and 3′ UTRs, a protein-coding sequence region, and a poly(A) tail (of ~120 nt). In this study, the designed mRNAs used the Cap1 structure, and human and mouse alpha globin sequences were selected as the 5′ and 3′ UTRs of the mRNA sequences, respectively. These sequences have been reported to promote efficient expression [28]. From this basic sequence, we continued optimization of the RNA construct to improve MG1113 expression.

To determine the most efficient mRNA design for in vitro MG1113 IgG4 antibody production, we compared monocistronic and polycistronic formats. In the monocistronic design, separate mRNAs were used for the heavy chain (HC) and LC, whereas the polycistronic format co-expressed both chains in a single transcript using T2A or P2A self-cleaving sequences (Fig. 1A). Various mRNA constructs were transfected into HEK293 and Huh7 cells, and antibody concentrations in the culture supernatants were quantified by ELISA 24 h post-transfection (Fig. 1B). In both cell lines, monocistronic constructs produced substantially higher levels of MG1113 than polycistronic ones. Monocistronic co-transfection of HC- and LC-encoding mRNAs yielded the highest antibody expression levels in both cell lines, with concentrations exceeding 150 ng/mL in Huh7 cells and 200 ng/mL in HEK293 cells. In contrast, polycistronic constructs encoding HC and LC separated by either T2A or P2A sequences exhibited significantly lower antibody expression. Among the polycistronic groups, the P2A-linked construct performed slightly better than the T2A-linked one, which is consistent with previous findings [29]. These results suggest that the monocistronic approach, using separate mRNAs for HC and LC, is more efficient for MG1113 antibody production than the polycistronic one.

To further evaluate the performance of monocistronic mRNA constructs for MG1113 antibody expression, in vitro experiments were conducted using Huh7 cells. In vitro-transcribed (IVT) mRNAs encoding the HC and LC of MG1113 were transfected into the cells, and the antibody concentrations in the culture supernatant were quantified by ELISA 24 and 48 h later (Fig. 1C). A clear dose-dependent increase in antibody production was observed, indicating successful production and secretion of MG1113 IgG4 antibodies. To confirm the size and assembly of the expressed antibody, the supernatants from transfected Huh7 cells were analyzed by SDS-PAGE and western blotting under nonreducing conditions (Supplementary Fig. 2A and 2B). The results revealed a clear band at approximately 150 kDa, which was consistent with the expected size of the full-length IgG. Using an anti-human Fc-HRP-conjugated antibody, the assembled IgG4 form of MG1113 was specifically detected, and the band intensity increased in a dose-dependent manner according to the amount of mRNA transfected. These results confirmed that the mRNA-encoded MG1113 antibody was not only successfully expressed and secreted in vitro, but also correctly assembled into a structurally intact IgG4 form.

Most secretory proteins contain a short amino acid sequence at the N-terminus known as a signal peptide (SP) sequence. The SP is crucial for the translocation of secretory proteins into the endoplasmic reticulum and the subsequent release of proteins extracellularly. Here, we assessed various SPs to determine their effectiveness in enhancing the secretion levels of the MG1113 antibody. To identify the most efficient SP for MG1113 expression, we compared IVT mRNA synthesized with MG1113, naïve (IGHV3, IGKV2), IgE, or hIgLCk SP (Fig. 1D). IVT mRNA encoding the HC and LC of MG1113 corresponding to four types of signal peptides was synthesized. Subsequently, HEK293 cells were transfected with MG1113 mRNA containing various SPs, and MG1113 concentrations in the cell media were measured by ELISA. Although intracellular levels of MG1113 were unaffected by the SP sequence, we found that mRNA containing the MG1113 SP resulted in higher levels of MG1113 in the cell medium compared with naïve (IGHV3, IGKV2), IgE, and hIgLCk SPs (Fig. 1E). In all subsequent studies, MG1113 mRNA was thus analyzed using the MG1113 SP.

2.2. Optimization of mRNA for optimal MG1113 antibody expression in vitro and in vivo

We optimized three key components to achieve maximal MG1113 expression in vitro and in vivo. First, we adjusted the mRNA ratio of the antibody heavy chain (HC) and light chain (LC). The HC of IgG antibodies is generally twice as long as the LC. The associated difference in mRNA length may lead to variations in translation efficiency and assembly. We thus investigated the translation efficiency based on the HC:LC ratio. Huh7 cells were transfected with varying HC:LC ratios (0.5:1, 1:1, 2:1, 4:1, and 8:1), and antibody expression was assessed (Fig. 2A). The results revealed that the HC:LC ratio of 1:1 produced higher antibody levels than the other ratios (0.5:1, 2:1, 4:1, and 8:1), confirming that an equal ratio of HC- and LC-encoding mRNA supports optimal antibody assembly [30]. Additionally, to evaluate the in vivo translation efficiency of MG1113 based on the HC:LC ratio, MG1113 mRNA was formulated into lipid nanoparticles (LNPs). The physicochemical characteristics of the LNPs were assessed using a Zetasizer Nano ZS and RiboGreen assay. The LNP-MG1113 mRNA exhibited an average particle size of 60 nm with a polydispersity index (PDI) of less than 0.1. The encapsulation efficiency, determined by the RiboGreen assay, was about 93 % (Fig. 2B**)**. We then compared the serum concentrations of MG1113 in C57BL/6 mice intravenously administered with MG1113 mRNA/LNPs prepared at different HC:LC ratios. Among the ratios tested, the 1:1 ratio yielded the highest serum concentration (Fig. 2C), which was consistent with the results from in vitro studies. Based on these findings, an HC:LC mRNA ratio of 1:1 was adopted for subsequent experiments.

Second, to optimize the translation efficiency of MG1113 mRNA, we evaluated combinations of 5′ and 3′ untranslated regions (UTRs) which are known to influence mRNA stability and translational output. In this study, four different 5′ UTRs (human HBA, IGHV3–23, γ-globin, and synthetic HBA) were combined with four 3′ UTRs (mouse HBA, human HBA, AES-mtRNR, and human IGKC) and inserted into monocistronic mRNA constructs encoding MG1113 (Fig. 2D and Supplementary Table 1). Six IVT mRNAs variants generated from these UTR combinations were transfected into Huh7 cells, and MG1113 antibody expression levels were measured 24 h after transfection. The results indicated that the UTR combination Db (5′ UTR: synthetic HBA, 3′ UTR: human HBA) resulted in significantly higher MG1113 antibody expression than for all other UTR combinations (Fig. 2E). In addition, to further assess translation efficiency in vivo, MG1113 mRNA was formulated into lipid nanoparticles (LNPs). The physicochemical properties of resulting LNPs were measured using a Zetasizer Nano ZS and RiboGreen assay. The LNP-MG1113 mRNA displayed an average particle size of 60–96 nm with a polydispersity index (PDI) below 0.1. The encapsulation efficiency, determined by the RiboGreen assay, ranged from approximately 89 % to 97 % (Fig. 2F**)**. The MG1113 mRNA/LNPs were intravenously injected into C57BL/6 mice at a dosage of 0.35 mg/kg, and serum was analyzed 24 h after injection (Fig. 2G). Consistent with the in vitro findings, UTR combination Db again generated the highest serum MG1113 levels among all tested variants (Fig. 2H**)**. Notably, the combination with AES-mtRNR 3′ UTR — a synthetic 3′ untranslated region reported to enhance mRNA stability and translations—showed the lowest expression in this system [31]. These results collectively demonstrate that pairing the synthetic HBA 5′ UTR with the human HBA 3′ UTR markedly improves the translation efficiency of MG1113 mRNA. These findings also underscore the critical roles of both 5′ and 3′ UTRs in modulating mRNA translation and stability, which aligns with prior research [31–33].

Finally, to evaluate the impact of sequence design and chemical modifications on mRNA quality, we assessed the integrity and presence of double-stranded RNA (dsRNA) in IVT MG1113 mRNA using dot blotting and denaturing gel electrophoresis (Fig. 3A). Clear bands corresponding to the HC and LC were observed in both standard mRNA and uridine-depleted (ud) mRNA, indicating that the transcribed mRNA was intact. Dot blot analysis showed that standard mRNA synthesized with

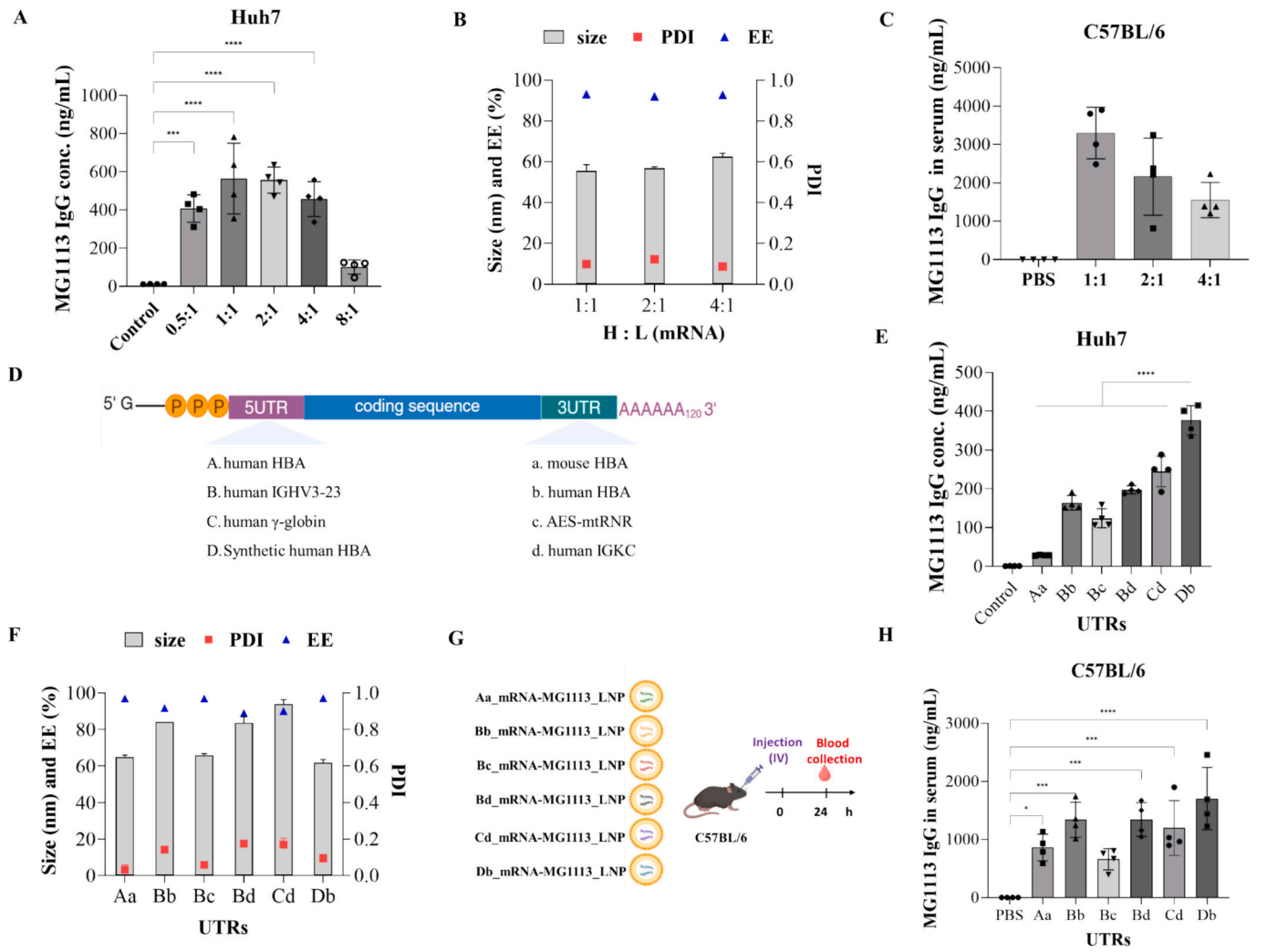


Fig. 2. Optimization of mRNA for optimal MG1113 antibody expression in vitro and in vivo. (A) MG1113 expression in Huh7 cells at varying HC:LC mRNA ratios (0.5:1, 1:1, 2:1, 4:1, 8:1). (B) Physicochemical properties of MG1113 mRNA-LNP formulated at different HC:LC ratios. Encapsulation efficiency, particle size, and polydispersity index (PDI) were measured using a RiboGreen assay and dynamic light scattering (DLS). (C) In vivo MG1113 antibody expression in C57BL/6 mice 24 h post-injection of LNP-formulated mRNAs at HC:LC ratios of 1:1, 2:1, and 4:1(0.35 mg/kg). (D) Schematic of monocistronic mRNA constructs incorporating various 5′ UTR (A–D) and 3′ UTR (a–d) combinations. (E) MG1113 antibody concentrations in Huh7 cell culture supernatants 24 h post-transfection with different UTR combinations. (F) Physicochemical characterization of MG1113 mRNA-LNP formulations with different 3'UTRs. (G) Experimental design for in vivo evaluation. (H) MG1113 concentrations in the serum of C57BL/6 mice one day after intravenous injection of LNP-formulated IVT-mRNAs containing the tested UTR combinations. Data are shown as mean ± SEM ($n = 2$–4). Statistical analyses were performed using one-way ANOVA with Tukey's post hoc test. Asterisks denote statistical significance (*$p < 0.05$, **$p < 0.01$, ***$p < 0.001$, ****$p < 0.0001$).

N1-methylpseudouridine (m1Ψ) showed relatively high level of dsRNA, whereas uridine-depleted mRNA substituted with 5-methoxyuridine (5moU) showed substantially reduced dsRNA signals [34]. These findings suggest that combining uridine depletion with alternative nucleoside substitutions effectively reduces immunogenic by-products generated during mRNA production.

Furthermore, we transfected Huh7 cells with four mRNA variants—st_Db(m1Ψ), ud_Db(m1Ψ), st_Db(5moU), and ud_Db(5moU)— to evaluate their differences in in vitro expression and measured MG1113 antibody levels in the culture supernatant 24 h after transfection. The results showed that the ud_Db(5moU) group achieved the highest antibody expression at a concentration of approximately 500 ng/mL, which was significantly greater than those of the other groups (Fig. 3B). Uridine depletion alone improved the expression of uridine, and its combination with 5-methoxyuridine (5moU) exerted a synergistic effect. These results demonstrate that specific nucleoside substitutions and uridine depletion can significantly enhance the efficiency of mRNA translation [35,36].

To validate these findings in vivo, MG1113 mRNA was encapsulated into LNPs formulated with different nucleoside combinations. The physicochemical characteristics of the resulting LNPs were assessed using a Zetasizer Nano ZS and RiboGreen assay. LNP-MG1113 mRNA exhibited an average particle size of 62–66 nm with a polydispersity index (PDI) of less than 0.1. The encapsulation efficiency, determined by the RiboGreen assay, ranged from 95 % to 96 % (Fig. 3C). Formulated LNP-MG1113 mRNA was then intravenously administered to C57BL/6 mice at a dose of 1 mg/kg. Consistent with in vitro screening, serum MG1113 IgG concentrations measured 24 h post-injection were highest in the ud_Db(m1Ψ) group, reaching approximately 30,000 ng/mL, which was significantly greater than the ~20,000 ng/mL observed in the ud_Db(5moU) group (Fig. 3D). However, contrary to the in vitro results the combination of uridine depletion and N1-methylpseudouridine (m1Ψ) substitution proved more effective in elevating the in vivo expression levels of MG1113 mRNA. These differences between in vitro and in vivo expression patterns may reflect distinct dynamics in ribosomal recruitment, recycling or modification-dependent decoding, as

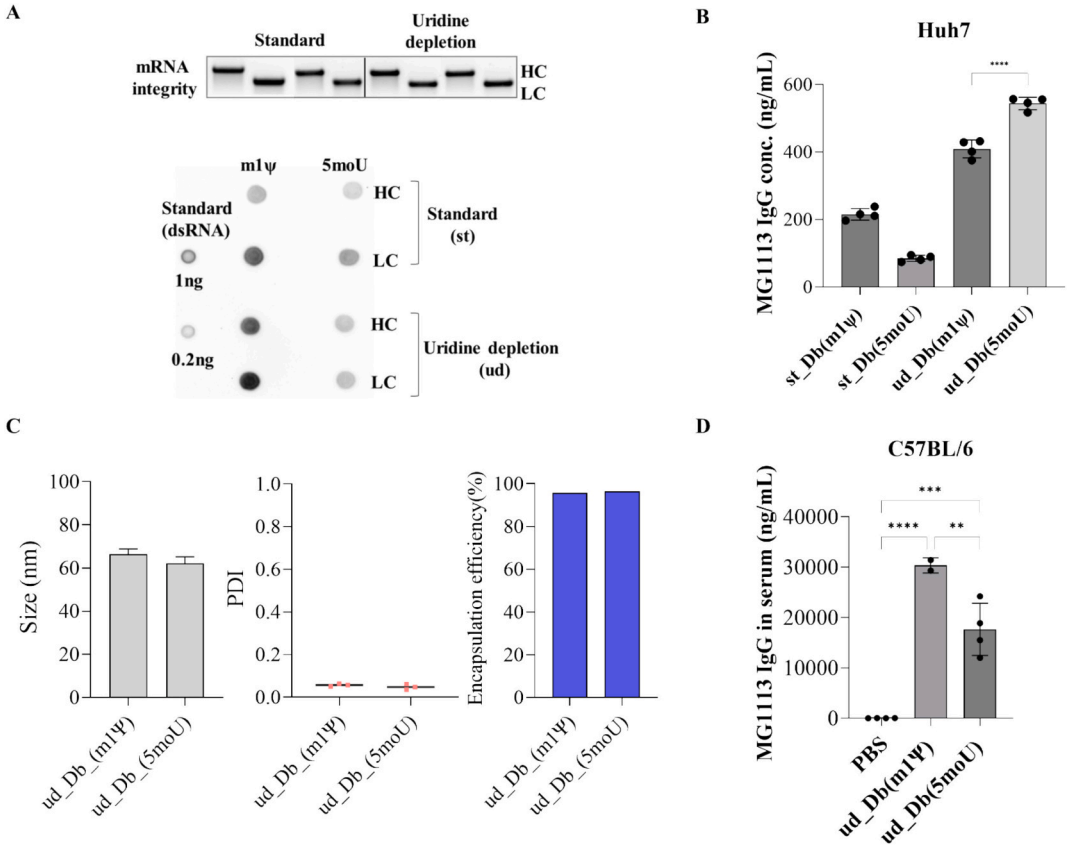


Fig. 3. Impact of codon optimization, uridine depletion, and nucleoside modification on mRNA-based MG1113 antibody production. (A) mRNA integrity confirmed by 1 % denaturing gel (top) and dsRNA content assessed by dot blot for mRNAs incorporating 5-methoxyuridine (5moU) and N1-methylpseudouridine (m1Ψ) (bottom). (B) MG1113 production in Huh7 cells 24 h post-transfection with four mRNA variants: standard codon usage with or without 5moU, and uridine-depleted (ud) sequences with or without 5moU. (C) Physicochemical characterization of MG1113 mRNA-LNP formulations with different nucleoside modification. (D) Serum MG1113 concentrations in C57BL/6 mice 24 h post-injection of LNP-formulated mRNA (1 mg/kg). Data are shown as mean ± SEM (n = 2–4). Statistical analyses were performed using one-way ANOVA with Tukey's post hoc test. Asterisks denote statistical significance (**p < 0.01, ***p < 0.001, ****p < 0.0001).

previously reported [36–38]. Notably, N1-methylpseudouridine (m1Ψ) has been shown to enhance ribosomal accuracy and translation efficiency under physiological conditions, which may contribute to its superior in vivo performance [38–41]. These findings highlight the importance of evaluating nucleotide modifications in both in vitro and in vivo settings for the rational optimization of mRNA therapeutics. Building on these findings, we next evaluated the in vivo pharmacokinetic and pharmacodynamic profiles of the optimized mRNA-MG1113 and compared them with those of the recombinant MG1113 antibody.

2.3. Pharmacokinetic analysis of optimized mRNA-encoded MG1113 compared with recombinant MG1113 antibody in mice

To evaluate the dose-dependent expression of mRNA-based MG1113, mRNA-MG1113 was synthesized in vitro and quality-checked by denaturing agarose gel analysis (Supplementary Fig. 1), after which it was formulated into LNPs. Using a Zetasizer Nano ZS and RiboGreen assay, the physicochemical properties of the LNPs were evaluated. The LNP-MG1113 mRNA displayed an average particle diameter of approximately 66 nm with a polydispersity index (PDI) below 0.1, and the RiboGreen assay further confirmed an encapsulation efficacy of roughly 96 % (Fig. 4A). These LNPs were intravenously administered to C57BL/6 mice at doses of 0.5, 1, and 2 mg/kg. Serum MG1113 IgG concentrations were measured 24 h after injection. The results showed a dose-dependent increase in antibody expression (Fig. 4B). Significantly, the group receiving 2 mg/kg presented approximately 60,000 ng/mL of antibody, which was higher than the levels in the 0.5 and 1 mg/kg groups. This indicates that increasing the mRNA dosage was closely associated with enhanced in vivo antibody expression.

Subsequently, to compare the pharmacokinetic profiles of mRNA-encoded MG1113 with those of the recombinant MG1113 antibody, mRNA-MG1113/LNPs were intravenously administered to C57BL/6 mice at doses of 1 mg/kg and 2 mg/kg. Recombinant MG1113 antibody was administered at 2 mg/kg via either subcutaneous or intravenous injection for comparison with the mRNA formulation. Serum antibody concentrations were then measured 5 min, 20 min and 1 h for MG1113 antibody and 0.25, 1, 2, 7, 14, and 21 days for all after injection (Fig. 4C).

As shown in Fig. 4D, both mRNA doses resulted in rapid increases in serum MG1113 levels, reaching peak concentrations within 24 h post-administration. The 2 mg/kg mRNA group revealed the highest peak concentration, approaching nearly 60,000 ng/mL, whereas the 1 mg/kg group produced approximately 20,000 ng/mL at the same time point. In contrast, direct administration of recombinant MG1113 antibody (2 mg/kg, IV or SC) generated substantially lower serum antibody levels throughout the study period. Although all groups showed gradual declines thereafter, mRNA-treated mice maintained higher MG1113 concentrations over the 21-day assessment window compared with protein-treated controls (Fig. 4D).

Consistent with these findings, AUC analysis demonstrated that the 2 mg/kg mRNA-MG1113 group exhibited the greatest overall exposure, with an AUC exceeding 9×10^6 ng·mL^{-1}·day, which was more than twofold higher than that of recombinant MG1113 antibody administered intravenously (Fig. 4E). The 1 mg/kg mRNA group and recombinant antibody groups showed markedly lower AUC values, further confirming that mRNA delivery produced superior systemic MG1113

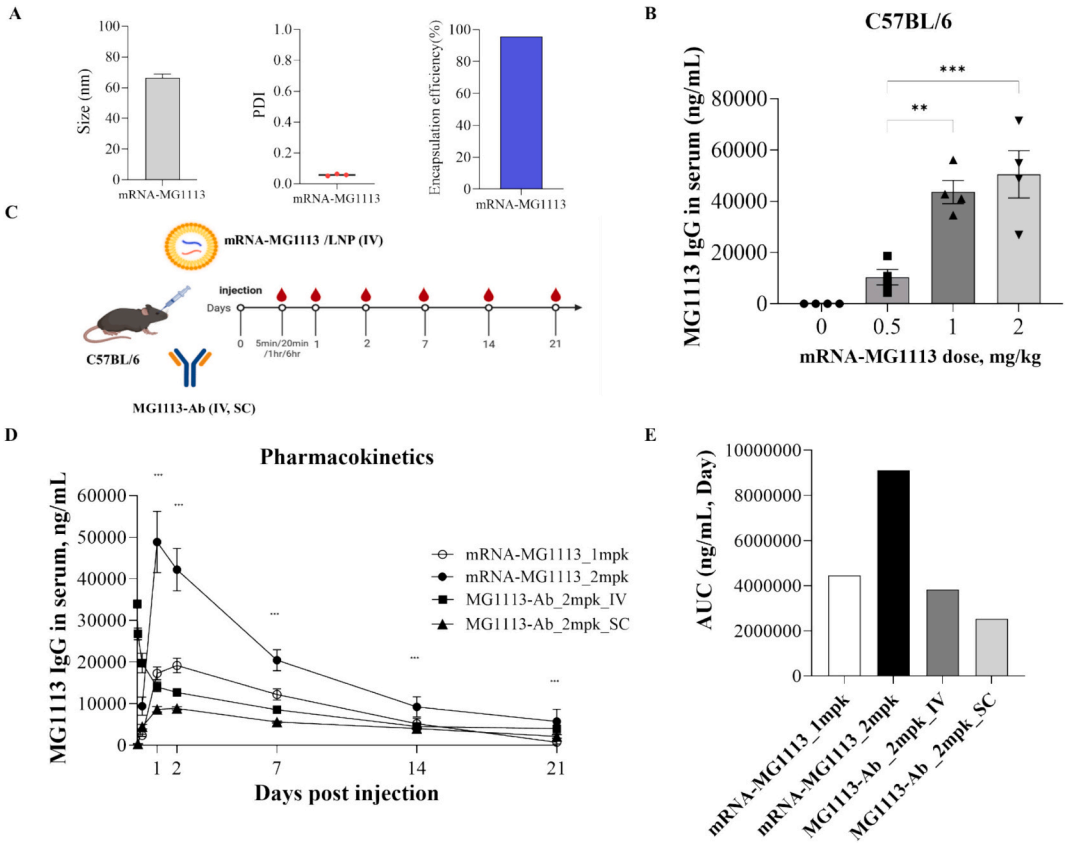


Fig. 4. Dose-dependent expression and pharmacokinetic comparison of mRNA-MG1113 versus recombinant MG1113 antibody. (A) Physicochemical properties of MG1113 mRNA-LNP formulations. Encapsulation efficiency, particle size, and polydispersity index (PDI) were measured using a RiboGreen assay and dynamic light scattering (DLS). (B) Serum MG1113 concentrations in C57BL/6 mice 24 h after intravenous administration of LNP-formulated mRNA-MG1113 at doses of 0.5, 1, and 2 mg/kg. (C) Schematic representation of the single-dose pharmacokinetic study comparing mRNA-encoded MG1113 with the recombinant MG1113 antibody. (D) Serum concentrations of MG1113 IgG after a single dose of mRNA-MG1113/LNP (1 or 2 mg/kg; open or closed circles) or recombinant MG1113 antibody delivered intravenously (2 mg/kg; squares) or subcutaneously (2 mg/kg; triangles). Concentrations were monitored for 21 days ($n = 4$). Serum concentrations were measured at early time points(5 min, 20 min and 1 h) for MG1113-Ab and on days 0.25, 1, 2, 7, 14, and 21 for all. (E) Comparison of AUC values between mRNA-encoded MG1113 and recombinant MG1113 antibody. Data are mean ± SEM (n = 4); two-way repeated-measures ANOVA with Sidak's post hoc test (**p < 0.01, ***p < 0.001, ****p < 0.0001).

exposure. Together, these results show that a single IV dose of mRNA-MG1113/LNP achieves substantially higher peak serum concentrations and overall systemic exposure of MG1113 antibody compared with direct antibody administration, demonstrating the pharmacokinetic advantage of mRNA-encoded antibody delivery.

Additionally, serum cytokine analysis at 24 h post-injection revealed no significant differences in mIL-6 or mTNF-α levels between the mRNA-MG1113 and protein MG1113 groups, indicating a low systemic inflammatory response (Supplementary Fig. 3A and Fig. 3B). These results show that the optimized mRNA not only increases expression in a dose-dependent manner but also induces significantly longer-lasting in vivo antibody exposure compared with the recombinant protein. These results also demonstrate comparable immunogenicity, confirming that this approach with high mRNA doses of up to 2 mg/kg is safe.

2.4. Evaluation of mRNA-MG1113 expression and liver toxicity after multiple administrations in mice

As most therapeutics are administered repeatedly rather than as a single dose, mRNA-encoded MG1113 was also evaluated through repeated dosing to assess the durability of its effect and its safety.

Prior to administration, mRNA-MG1113 was formulated into lipid nanoparticles (LNPs), which consistently demonstrated uniform physicochemical properties across three independent preparations. The encapsulation efficiency remained high at 95–96 %, particle sizes were distributed within the 66–73 nm range, and the PDI values were below 0.15, indicating stable and reproducible LNP formation (Fig. 5A).

To evaluate pharmacokinetics and tolerability following repeated intravenous administration, C57BL/6 mice received mRNA-MG1113/LNPs at a dose of 1 mg/kg on days 0, 7, and 14 (Fig. 5B). Serum samples were periodically collected for MG1113 IgG quantification and liver enzyme analysis. Serum MG1113 levels exhibited similar expression profiles after each dosing event, characterized by a rapid increase that peaked at 24 h post-injection and gradually declined until the next administration (Fig. 5C). All three injections produced comparable expression levels, demonstrating reproducible in vivo translation.

In addition, liver toxicity markers were evaluated 24 h after dosing and remained within acceptable ranges throughout the study period. A transient increase in AST was observed after the first administration but returned to baseline by day 8, and ALT levels also remained largely unchanged at all time points (Fig. 5D). These results indicate that repeated intravenous administration mRNA-MG1113/LNPs is well tolerated and does not induce significant hepatic toxicity. Overall, repeated dosing of mRNA-MG1113/LNPs in mice demonstrates sustained expression of a TFPI-binding antibody without any signs of systemic or hepatic toxicity.

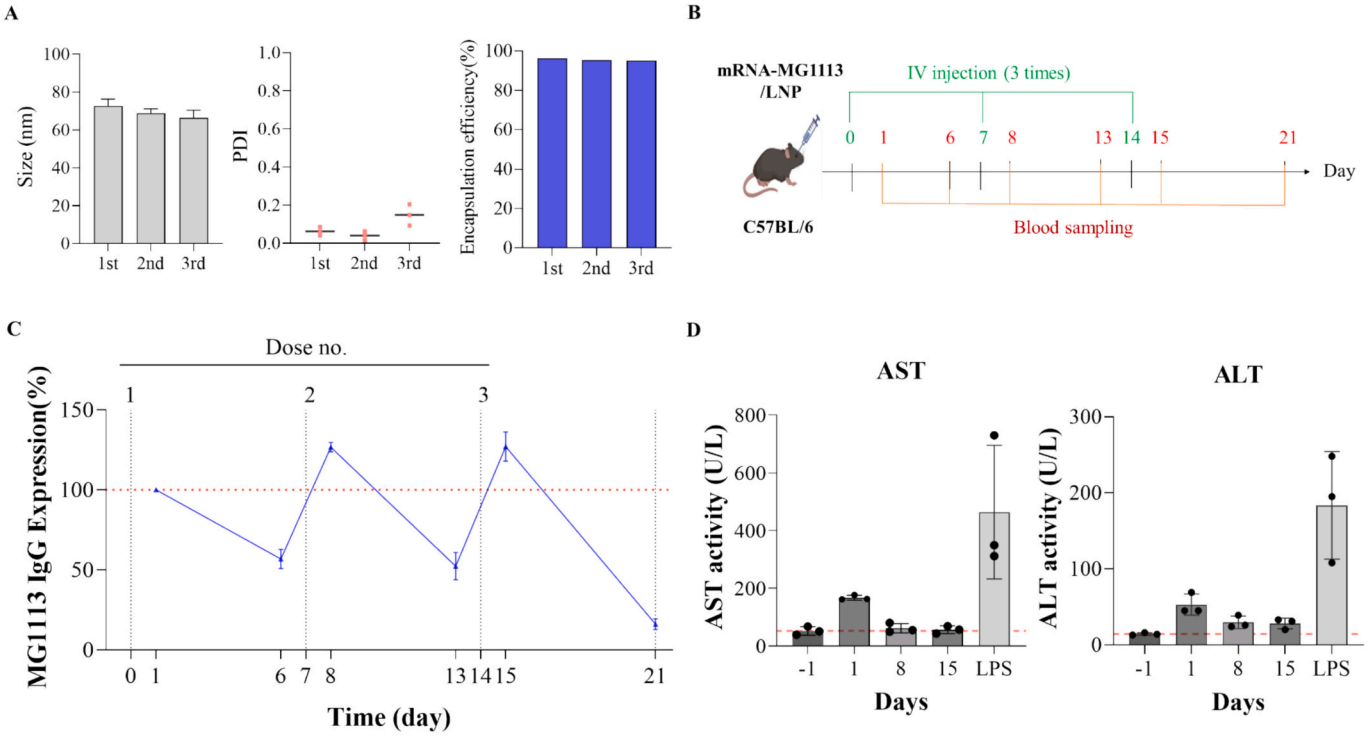


Fig. 5. Repeated dosing and liver toxicity of mRNA-MG1113. (A) Physicochemical characterization of three independently prepared mRNA-MG1113/LNP formulations. Encapsulation efficiency, particle size, and polydispersity index (PDI) were measured using a RiboGreen assay and dynamic light scattering (DLS). (B) Schematic of the repeated-dose study design. Mice received mRNA-MG1113/LNP intravenously on Days 0, 7 and 14 followed by serum collection through Day 21. (C) Serum MG1113 IgG expression profiles following repeated intravenous dosing of mRNA-MG1113/LNP(1 mg/kg). (D) Serum AST and ALT levels measured after repeated dosing to evaluate hepatic safety. Positive control group was injected 10 mg/kg of lipopolysaccharide. Data are mean ± SEM ($n = 3$).

2.5. Comparison of duration of TFPI suppression using optimized mRNA-encoded MG1113 and recombinant antibody in rabbits

To evaluate the pharmacological relationship between the MG1113 antibody and its target protein, free TFPI, optimized mRNA-MG1113 was encapsulated into LNPs that displayed high encapsulation efficiency and uniform particle size (Fig. 6A). The mRNA-MG1113/LNPs xhibited a uniform particle size of approximately 63 nm with a low polydispersity index (PDI < 0.05) and an encapsulation efficiency of 93 %, confirming their suitability for systemic administration. The overall rabbit study design is shown in Fig. 6B, in which a single intravenous dose of mRNA-MG1113 (2 mg/kg) or recombinant MG1113 antibody (2 mg/kg) was administered, followed by serial measurements of pharmacokinetic and pharmacodynamic parameters.

As shown in Fig. 6C, serum MG1113 levels increased rapidly in both groups during the first 24 h after dosing. The recombinant antibody reached a substantially higher initial concentration, reflecting the immediate systemic availability of the purified protein. In contrast, mRNA-MG1113 produced lower early antibody levels but maintained a more gradual decline, indicating sustained in vivo antibody production from mRNA translation rather than rapid clearance of a bolus protein dose.

Despite these lower circulating antibody concentrations, mRNA-MG1113 induced a more durable pharmacodynamic response. Free TFPI concentrations were markedly reduced within 24 h of mRNA-MG1113 administration and remained strongly suppressed through day 14, with partial recovery by day 21 (Fig. 6D). In comparison, TFPI levels in the recombinant antibody group rebounded more rapidly and fluctuated throughout the study, demonstrating shorter-lived pharmacodynamic activity.

To further assess functional coagulation outcomes, clotting time was evaluated using the modified prothrombin time (mPT) assay (Supplementary Fig. 4). Consistent with TFPI suppression, rabbits treated with mRNA-MG1113 showed a more sustained reduction in mPT over the 21-day period. Whereas mPT values in the recombinant antibody group began to normalize soon after dosing, the mRNA-MG1113 group maintained prolonged increases in coagulation activity (lower mPT) until approximately day 14, with gradual return toward baseline thereafter. These findings indicate that continuous endogenous production of MG1113 mediated by mRNA-LNPs results in extended pharmacodynamic efficacy that surpasses the duration achieved by bolus recombinant antibody administration.

Collectively, these results demonstrate that mRNA-mediated delivery of MG1113 enables sustained antibody exposure and prolonged functional inhibition of TFPI, supporting the potential of mRNA-LNP platforms as a long-acting therapeutic modality.

3. Discussion

Hemophilia is a hereditary bleeding disorder caused by deficiencies or dysfunctions in coagulation factor VIII (hemophilia A) or IX (hemophilia B), most commonly arising from mutations in X-linked genes. Although the prophylactic administration of recombinant or plasma-derived clotting factors has significantly improved clinical outcomes, this approach remains limited by the need for frequent intravenous dosing, the high treatment burden, and the emergence of inhibitory antibodies that compromise efficacy and patient compliance [1,2]. These limitations highlight the urgent need for alternative therapeutic platforms that provide improved durability, reduced immunogenicity, and enhanced accessibility.

To address these issues, we have developed a synthetic mRNA-LNP therapeutic system for the in vivo production of MG1113, a humanized monoclonal antibody targeting TFPI. This approach, which replaces external protein delivery with endogenous synthesis, holds the potential to overcome the major drawbacks of conventional biopharmaceuticals. To substantiate this potential, our research involved the systematic optimization of the MG1113 mRNA and its delivery system. We first

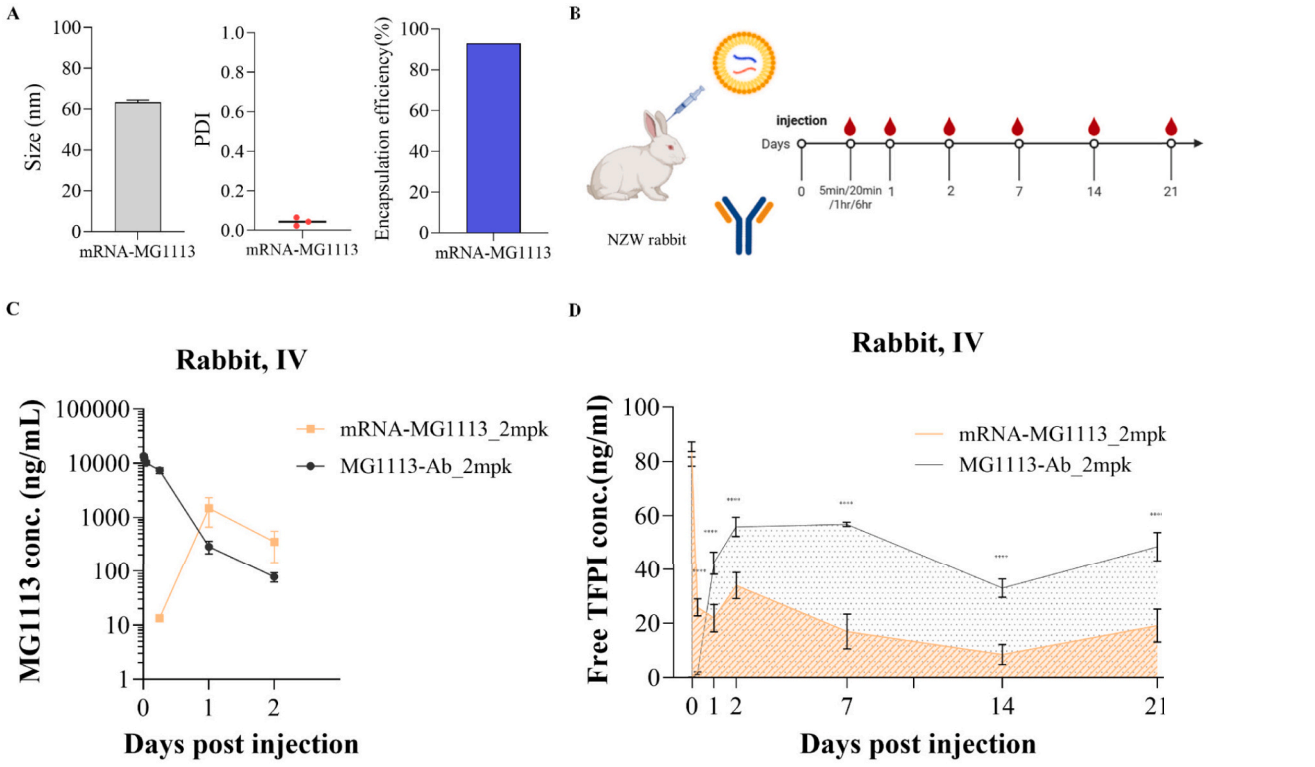


Fig. 6. Plasma concentration–time profiles of MG1113 IgG4 and free TFPI in rabbits following administration of mRNA-encoded versus recombinant MG1113. (A) Physicochemical characterization of MG1113 mRNA-LNP formulations. Encapsulation efficiency, particle size, and polydispersity index (PDI) were measured using a RiboGreen assay and dynamic light scattering (DLS). (B) Schematic representation of the in vivo study design in rabbits. (C) Plasma MG1113 level profiles after intravenous injection of LNP-formulated MG1113 mRNA (2 mg/kg) and MG1113-Ab(2 mg/kg). The concentration of MG1113 was determined by ELISA. MG1113 levels beyond day 2 were not quantified due to assay limitations. Limit of Quantitation (LOQ). (D) Plasma Free TFPI profiles after intravenous injection of LNP-formulated mRNA-MG1113(2 mg/kg) and MG1113-Ab(2 mg/kg). Free TFPI concentrations were analyzed by ELISA. Data are presented as the mean ± SEM (n = 4). Statistical analyses were performed using two-way ANOVA with Tukey's post hoc test. Asterisks denote statistical significance (****$p < 0.0001$).

determined that a monocistronic design, encoding the heavy and light chains on separate mRNAs, yielded significantly higher antibody production in both HEK293 and Huh7 cells than a bicistronic format. Furthermore, we identified that a 1:1 ratio of mRNAs encoding the heavy and light chains was optimal for expression and assembly. Additionally, through UTR screening, we confirmed that the combination of a synthetic HBA 5' UTR and the human HBA 3' UTR was the most effective pairing for enhancing translation, suggesting that UTR efficacy is highly context-dependent and requires validation for each coding sequence.

Building on this optimized construct, we integrated chemical modifications such as codon optimization, uridine depletion, and the incorporation of N1-methylpseudouridine to further promote mRNA translation and evade recognition by the innate immune system. These modifications contributed to increased expression and extended pharmacodynamic activity in vivo. Moreover, in a direct comparison with the recombinant protein, the mRNA-LNP delivery method achieved higher and more sustained plasma concentrations of MG1113, demonstrating that intracellular synthesis can significantly improve its pharmacokinetics.

The distinct pharmacokinetic profiles of mRNA-based MG1113 and recombinant MG1113 appear to account for their differences in pharmacodynamic effects. Recombinant MG1113 reached a high initial concentration immediately after administration but was rapidly cleared, resulting in a rebound increase in free TFPI levels by day two. In contrast, mRNA-MG1113 induced continuous antibody production, allowing for gradual accumulation and prolonged persistence in the serum. This is likely because LNPs are preferentially taken up by the liver, where the delivered mRNA is locally translated within hepatocytes and the surrounding vascular microenvironment, providing a sustained source of antibody production. This sustained exposure appears to maintain a functionally meaningful antibody concentration within the hepatic and vascular microenvironment, enabling durable suppression of free TFPI for up to 14 days. Consistent with these findings, the mPT analysis showed that mRNA-MG1113 induced a more gradual and sustained improvement in coagulation activity over 21 days, in contrast to the transient effect of the recombinant antibody.

However, this study has several limitations. While pharmacological activity was supported by a reduction in free TFPI and an improvement in mPT, direct hemostatic efficacy was not assessed in a hemophilia model, which limits our ability to draw definitive therapeutic conclusions. Moreover, uncertainties regarding the clearance dynamics of TFPI–antibody complexes and potential differences in tissue distribution remain unresolved challenges. Follow-up studies utilizing species-appropriate disease models and integrated PK/PD analysis are necessary to fully elucidate the therapeutic potential of this approach. Nevertheless, our findings provide a robust proof-of-concept that mRNA-LNP delivery enables the in vivo production of a functional anti-TFPI antibody with sustained pharmacological activity.

In conclusion, our findings demonstrate that mRNA-LNP delivery enables the in vivo production of a functional anti-TFPI antibody with sustained pharmacological activity. The prolonged antibody expression and durable TFPI suppression support the feasibility of mRNA-encoded MG1113 as a long-acting therapeutic. This approach simplifies manufacturing and may reduce dosing frequency compared with recombinant antibodies. Overall, these results establish mRNA-LNPs as a promising next-generation platform for antibody-based therapies and highlight the need for further validation in hemophilia models.

4. Materials and methods

4.1. Plasmid construction and in vitro mRNA transcription

DNA sequences encoding the heavy chain (HC) and LC of the MG1113 IgG4 antibody were codon-optimized for human expression using GeneArt (Thermo Fisher Scientific, Waltham, MA, USA). Sequences were designed with or without uridine depletion and cloned into a T7 promoter-driven linearized plasmid backbone containing the necessary regulatory elements. The standard plasmid configuration included a 5′ untranslated region (UTR), SP, open reading frame (ORF), 3′ UTR, and 120 nt poly(A) tail. For UTR screening experiments, multiple 5′ UTRs (e.g., human HBA, IGHV3–23, synthetic HBA, γ-globin) and 3′ UTRs (e.g., human HBA, mouse HBA, hIGKC, AES-mtRNR) were cloned upstream and downstream of the ORF, respectively. IVT was performed using a MEGAscript™ T7 Transcription Kit (Thermo Fisher Scientific, AM1334). Reactions were set up to include cap analogs (CleanCap AG, N-7413) for cotranscriptional capping. N1-methylpseudouridine (m1Ψ) and 5-methoxyuridine (5moU) were substituted for uridine in modified constructs. The cap analogs, m1Ψ and 5moU, were purchased from TriLink BioTechnologies. IVT products were treated with DNase I to remove DNA templates and purified by LiCl precipitation or using the MEGAclear™ Transcription Clean-Up Kit (Thermo Fisher Scientific, AM1908). RNA quality was assessed using agarose gel electrophoresis and quantified via NanoDrop.

4.2. Lipid nanoparticle (LNP) formulation and characterization

LNPs were prepared using a microfluidic mixing method (NanoAssemblr Ignite; Precision Nanosystems). The lipid mixture consisted of ionizable lipid (SM102), DSPC (1,2-distearoyl-sn-glycero-3-phosphocholine), cholesterol, and DMG-PEG2000 (1,2-dimyristoyl-rac-glycero-3-methoxypolyethylene glycol-2000) at a molar ratio of 50:10:38.5:1.5. Lipids were dissolved in ethanol, whereas IVT mRNA was diluted in an aqueous buffer (10 mM citrate buffer, pH 3.0). The two phases were mixed at a flow rate ratio of 3:1 (aqueous:organic) under controlled conditions. The final formulation was dialyzed against PBS (pH 7.4) to remove ethanol and concentrate the nanoparticles. The particle size, polydispersity index (PDI), and zeta potential were measured using a Zetasizer Nano ZS (Malvern). The encapsulation efficiency was determined using the RiboGreen™ assay (Invitrogen). Only formulations with encapsulation efficiencies greater than 90 % were used in the in vitro and in vivo experiments.

4.3. Cell culture and in vitro transfection

HEK293T (ATCC CRL-11268) and Huh7 (JCRB0403) cells were cultured in high-glucose Dulbecco's Modified Eagle Medium (DMEM; Gibco) supplemented with 10 % heat-inactivated fetal bovine serum (FBS,HyClone), 1 % penicillin–streptomycin (Gibco), and 1 % non-essential amino acids (for Huh7). Cells were maintained at 37 °C in a humidified atmosphere with 5 % CO_2.

For transfection experiments, cells were seeded in 24-well plates at a density of 1×10^5 cells/well. The next day, IVT mRNA was transfected using Lipofectamine™ MessengerMAX (LMRNA003; Thermo Fisher Scientific), prepared in accordance with the manufacturer's protocol. mRNA doses ranged from 100 to 1000 ng/well, depending on the experiment. The culture supernatants were obtained 24 or 48 h after transfection and clarified by centrifugation (300 ×*g*, 5 min) before downstream analyses.

4.4. Enzyme-linked immunosorbent assay (ELISA) for MG1113 quantification

MG1113 IgG4 antibody concentrations in culture supernatants and animal plasma/serum samples were measured using an indirect ELISA specific for human IgG. High-binding 96-well plates (Corning Costar) were coated overnight at 4 °C with 1 μg/mL human TFPI protein (Acro Biosystem, TFI-H5226) in PBS. The plates were washed with PBST (0.05 % Tween-20 in PBS) and blocked with 1 % BSA in PBS for 1 h at room temperature. Samples and serial dilutions of purified MG1113 standard (GC Biopharma) were added in duplicate and incubated for 1 h at 37 °C. The plates were washed and incubated with HRP-conjugated anti-human IgG Fc-specific (1:10,000, A0170; Sigma-Aldrich) for 1 h, followed by SureBlue™ TMB 1-Component Microwell Peroxidase Substrate (5120–0077; Seracare). The reaction was stopped with TMB stop solution (5150–0021; Seracare), and absorbance was measured at 450 nm using a microplate reader (SpectraMax; Molecular Devices). The antibody concentration was determined using the standard curve.

4.5. Enzyme-linked immunosorbent assay (ELISA) for free TFPI quantification

Free TFPI concentrations in animal plasma samples were measured using a sandwich ELISA specific for MG1113. High-binding 96-well plates (Corning Costar) were coated overnight at 4 °C with 2 μg/mL MG1113 (GC Biopharma) in PBS. The plates were washed with PBST (0.05 % Tween-20 in PBS) and blocked with 1 % BSA in PBS for 1 h at room temperature. Samples and serial dilutions of purified rabbit TFPI protein (HY-P700431; MEC) were added in duplicate and incubated for 1 h at 37 °C. The plates were washed and incubated with 100 μL of 0.1 μg/mL biotin-linked anti-human TFPI polyclonal Ab (BAF2974; R&D Systems) for 1 h. After washing, 100 μL of 1:10,000 diluted Streptavidin−Peroxidase Polymer, Ultrasensitive (S2438; Sigma-Aldrich), was added and incubated for 30 min. After washing, SureBlue™ TMB 1-Component Microwell Peroxidase Substrate (5120–0077; Seracare) was added and incubated for 10 min. The reaction was stopped with TMB stop solution (5150–0021; Seracare), and absorbance was measured at 450 nm using a microplate reader (SpectraMax; Molecular Devices). The antibody concentration was determined using the standard curve.

4.6. Western blotting and SDS-PAGE analysis

To verify the expression and integrity of MG1113 antibody, culture supernatants were analyzed using SDS-PAGE and immunoblotting. Proteins were denatured under nonreducing conditions in NuPAGE™ LDS Sample Buffer (4×) (NP0007; Invitrogen) and boiled for 5 min. Samples were resolved on NuPAGE™ 4 %–12 % Bis-Tris gels (Invitrogen) and transferred to PVDF membranes (Millipore). These membranes were then blocked in 5 % skim milk in TBST and probed with HRP-conjugated anti-human IgG Fc-specific Antibody (1:10,000, A0170; Sigma-Aldrich). Bands were visualized using Amersham™ ECL Detection Reagents and imaged on a ChemiDoc MP system.

4.7. Dot blot assay for detection of double-stranded RNA

To assess potential immunogenic contaminants in IVT mRNA, dot blotting was used to detect double-stranded RNA (10,080,100; Scicons). Equal amounts of purified mRNA (200 ng) were spotted onto a positively charged nylon membrane (11,417,240,001; Roche) and UV-crosslinked. Membranes were blocked with 5 % nonfat milk in TBST and incubated overnight with J2 monoclonal antibody (10,010,200; Scicons) specific for dsRNA. After washing, the membranes were incubated with Goat Anti-Mouse IgG H&L (HRP) (Abcam, ab97023) and developed using ECL.

4.8. Animal studies and in vivo analysis

Procedures for animal studies were approved by the Institutional Animal Care and Use Committee at Ewha Womans University. C57BL/6 male mice (6 to 8 weeks old) were purchased from Orient Bio (Korea)

and acclimated for 1 week. The mice were randomized and intravenously injected with MG1113 mRNA-LNPs at doses of 0.35, 0.5, 1, and 2 mg/kg or with 2 mg/kg recombinant MG1113 protein diluted in sterile PBS. Blood samples were collected retro-orbitally 5 min, 20 min, 1 and 6 h, and 1, 2, 7, 14, and 21 days after injection. Serum was isolated by centrifugation and stored at −80 °C until analysis by ELISA.

New Zealand White male rabbits (2 to 2.5 kg) were purchased from Koatech and individually raised in a well-controlled facility. The experiment was approved by the Institutional Animal Care and Use Committee of GC Biopharma. These rabbits received a single intravenous dose of MG1113 mRNA-LNPs or recombinant MG1113 antibody (2 mg/kg). Blood samples were collected from the marginal ear vein at baseline and 20 min, 1 and 6 h, and 1, 2, 7, 14, and 21 days later. MG1113 and free TFPI levels in plasma (02–683-172, BD Vacutainer® Citrate Tubes; Beckton Dickinson) were quantified by ELISA following the manufacturer's protocol. Free TFPI suppression was used as a surrogate marker of in vivo antibody activity.

4.9. Liver toxicity analysis for repeated dosing

Aspartate aminotransferase (AST) and Alanine aminotransferase (ALT) were measured using the clinical chemistry analyzer FUJI DRI-CHEM NX600V (FUJIFILM, Tokyo, Japan). Mice serum was separated and analyzed using the specific dry chemistry slides (DRI-CHEM Slide GOT/AST-P III and DRI-CHEM Slide GPT/ALT-P) according to the manufacturer's instructions.

4.10. Cytokine analysis in mouse serum

To assess systemic inflammatory responses following the administration of mRNA or protein therapeutics, serum cytokine levels were measured in C57BL/6 mice. Mice (6 to 8 weeks old, $n = 4$ per group) were intravenously injected with 2 mg/kg ud_Db_mRNA-MG1113 encapsulated in LNPs or with 2 mg/kg recombinant MG1113 antibody. The control animals were given an equivalent volume of PBS. Twenty-four hours after injection, blood was collected via retro-orbital bleeding and allowed to clot at room temperature. Serum samples were separated by centrifugation (3000 rpm, 10 min, 4 °C) and stored at −80 °C until analysis. The concentrations of mouse interleukin-6 (mIL-6) and tumor necrosis factor-alpha (mTNF-α) were quantified using commercially available ELISA kits (R&D Systems), in accordance with the manufacturer's protocols. Absorbance was measured at 450 nm using a microplate reader, and cytokine concentrations were calculated based on standard curves generated using recombinant standards.

4.11. Modified prothrombin time assay

A steel bead and 50 μL of plasma sample were added to each cuvette and incubated at 37 °C for 3 min. After the reaction, 100 μL of activator was added to each cuvette, and the clotting time was measured at 37 °C using the Start 4 Hemostasis Analyzer (Stago, Asnières sur Seine, France). The activator used was RecombiPlasTin 2G (Werfen, Barcelona, Spain), which was diluted to a 1:100,000 ratio using 0.025 M $CaCl_2$.

4.12. Statistical analysis

All quantitative data are presented as mean ± standard deviation (SD) or standard error of the mean (SEM), as indicated. Statistical analyses were performed using GraphPad Prism 9 software. One-way or two-way ANOVA was performed as appropriate, followed by Tukey's or Sidak's multiple comparison tests. A p-value of <0.05 was considered significant.

CRediT authorship contribution statement

Miyoung. Oh: Conceptualization, Data curation, Formal analysis, Methodology, Project administration, Supervision, Validation, Writing – original draft, Writing – review & editing. **Yujeong. Jeong:** Formal analysis, Investigation, Methodology, Validation. **Hyein. Jung:** Data curation, Formal analysis, Investigation, Methodology, Validation. **Yongjoo. Byeon:** Formal analysis, Investigation, Methodology. **Heechun. Kwak:** Formal analysis, Investigation, Methodology. **Songseop. Kim:** Investigation, Methodology, Validation. **Wonhyo. Seo:** Project administration, Supervision, Writing – review & editing. **Jaesung. Jung:** Project administration, Resources, Writing – review & editing. **Hyukjin. Lee:** Conceptualization, Project administration, Supervision, Writing – review & editing.

Declaration of competing interest

Miyoung Oh, Heechun Kwak, Songseop Kim and Jaesung Jung are employees of GC Biopharma.

Acknowledgements

This research was supported by GC Biopharma. This work was also supported by the Bio & Medical Technology Development Program of the National Research Foundation of Korea (NRF), funded by the Ministry of Science and ICT (MSIT) under the following grant numbers: RS-2023-00261343, RS-2024-00451880, RS-2024-00411768, RS-2025-00542986, RS-2024-00465298 and RS-2025-25455885. Schematic figures were created with BioRender.com.

Appendix A. Supplementary data

Supplementary data to this article can be found online at https://doi.org/10.1016/j.jconrel.2025.114520.

Data availability

Data will be made available on request.

References

[1] R. Peters, T. Harris, Advances and innovations in haemophilia treatment, Nat. Rev. Drug Discov. 17 (2018) 493–508.
[2] A.D. Shapiro, I.S. Mitchell, S. Nasr, The future of bypassing agents for hemophilia with inhibitors in the era of novel agents, J. Thromb. Haemost. 16 (2018) 2362–2374.
[3] R. Ljung, G. Auerswald, G. Benson, G. Dolan, A. Duffy, C. Hermans, V. Jimenez-Yuste, T. Lambert, M. Morfini, S. Zupancic-Salek, E. Santagostino, Inhibitors in haemophilia a and B: management of bleeds, inhibitor eradication and strategies for difficult-to-treat patients, Eur. J. Haematol. 102 (2019) 111–122.
[4] P.M. Mannucci, Hemophilia therapy: the future has begun, Haematologica 105 (2020) 545–553.
[5] Z. Wang, G. Wang, H. Lu, H. Li, M. Tang, A. Tong, Development of therapeutic antibodies for the treatment of diseases, Mol. Biomed. 3 (2022) 35.
[6] P.E. Alcedo Andrade, P.M. Mannucci, C.M. Kessler, Emicizumab: the hemophilia a game-changer, Haematologica 109 (2024) 1334–1347.
[7] K. Zhang, Lentiviral gene therapy with CD34+ hematopoietic cells for hemophilia a, N. Engl. J. Med. 392 (2025) 1765–1766.
[8] V. Muczynski, A.C. Nathwani, AAV mediated gene therapy for haemophilia B: from the early attempts to modern trials, Thromb. Res. 236 (2024) 242–249.
[9] D.S. Aschenbrenner, New treatment available for hemophilia A or B, Am. J. Nurs. 125 (2025) 20.
[10] S. Wichaiyo, Advances in development of drug treatment for hemophilia with inhibitors, ACS Pharmacol. Transl. Sci. 7 (2024) 3795–3803.
[11] J.P. Han, M. Kim, B.S. Choi, J.H. Lee, G.S. Lee, M. Jeong, Y. Lee, E.A. Kim, H.K. Oh, N. Go, H. Lee, K.J. Lee, U.G. Kim, J.Y. Lee, S. Kim, J. Chang, H. Lee, D.W. Song, S. C. Yeom, In vivo delivery of CRISPR-Cas9 using lipid nanoparticles enables antithrombin gene editing for sustainable hemophilia A and B therapy, Sci. Adv. 8 (2022) eabj6901.
[12] P. Chowdary, Anti-tissue factor pathway inhibitor (TFPI) therapy: a novel approach to the treatment of haemophilia, Int. J. Hematol. 111 (2020) 42–50.
[13] G. Castaman, V. Jimenez-Yuste, J. Mahlangu, Concizumab, a non-replacement therapy for persons with hemophilia with inhibitors, J. Clin. Med. 14 (2025).
[14] J. Mahlangu, J. Luis Lamas, J. Cristobal Morales, D.R. Malan, J. Teeter, R. J. Charnigo, E. Hwang, S. Arkin, Long-term safety and efficacy of the anti-tissue factor pathway inhibitor marstacimab in participants with severe haemophilia: phase II study results, Br. J. Haematol. 200 (2023) 240–248.

[15] S.C. Carrara, M. Ulitzka, J. Grzeschik, H. Kornmann, B. Hock, H. Kolmar, From cell line development to the formulated drug product: the art of manufacturing therapeutic monoclonal antibodies, Int. J. Pharm. 594 (2021) 120164.
[16] R. Kunert, D. Reinhart, Advances in recombinant antibody manufacturing, Appl. Microbiol. Biotechnol. 100 (2016) 3451–3461.
[17] F. Li, N. Vijayasankaran, A.Y. Shen, R. Kiss, A. Amanullah, Cell culture processes for monoclonal antibody production, MAbs 2 (2010) 466–479.
[18] H. Samaranayake, T. Wirth, D. Schenkwein, J.K. Raty, S. Yla-Herttuala, Challenges in monoclonal antibody-based therapies, Ann. Med. 41 (2009) 322–331.
[19] J.K. Liu, The history of monoclonal antibody development–progress, remaining challenges and future innovations, Ann. Med. Surg. 3 (2014) 113–116.
[20] M.L.D. Santos, W. Quintilio, T.M. Manieri, L.R. Tsuruta, A.M. Moro, Advances and challenges in therapeutic monoclonal antibodies drug development, Brazilian, J. Pharm. Sci. 54 (2018) e01007.
[21] N. Kose, J.M. Fox, G. Sapparapu, R. Bombardi, R.N. Tennekoon, A.D. De Silva, S. M. Elbashir, M.A. Theisen, E. Humphris-Narayanan, G. Ciaramella, A lipid-encapsulated mRNA encoding a potently neutralizing human monoclonal antibody protects against chikungunya infection, Sci. Immunol. 4 (2019) eaaw6647.
[22] Y. Rybakova, P.S. Kowalski, Y. Huang, J.T. Gonzalez, M.W. Heartlein, F. DeRosa, D. Delcassian, D.G. Anderson, mRNA delivery for therapeutic anti-HER2 antibody expression in vivo, Mol. Ther. 27 (2019) 1415–1423.
[23] A. Patel, M.A. Bah, D.B. Weiner, In vivo delivery of nucleic acid-encoded monoclonal antibodies, BioDrugs 34 (2020) 273–293.
[24] E. Narayanan, S. Falcone, S.M. Elbashir, H. Attarwala, K. Hassett, M.S. Seaman, A. Carfi, S. Himansu, Rational design and in vivo characterization of mRNA-encoded broadly neutralizing antibody combinations against HIV-1, Antibodies (Basel) 11 (2022).
[25] L. Wu, W. Wang, J. Tian, C. Qi, Z. Cai, W. Yan, S. Xuan, A. Shang, Intravenous delivery of RNA encoding anti-PD-1 human monoclonal antibody for treating intestinal cancer, J. Cancer 13 (2022) 579–588.
[26] H. Kwak, S. Lee, S. Jo, Y.E. Kwon, H. Kang, G. Choi, M.E. Jung, M.J. Kwak, S. Kim, B.H. Oh, D.S. Kim, S.H. Hwang, MG1113, a specific anti-tissue factor pathway inhibitor antibody, rebalances the coagulation system and promotes hemostasis in hemophilia, Res. Pract. Thromb. Haemost. 4 (2020) 1301–1312.
[27] E.Y. Kwak, M.J. Kim, J.H. Park, H.W. Jung, M.E. Jung, Target-mediated drug disposition modeling of an anti-TFPI antibody (MG1113) in cynomolgus monkeys to predict human pharmacokinetics and pharmacodynamics, J. Thromb. Haemost. 19 (2021) 1425–1435.
[28] P.K. Mandal, D.J. Rossi, Reprogramming human fibroblasts to pluripotency using modified mRNA, Nat. Protoc. 8 (2013) 568–582.
[29] Y.M. Li, M. Wang, T.Y. Wang, Y.G. Wei, X. Guo, C.L. Mi, C.P. Zhao, X.X. Cao, Y. Y. Dou, Effects of different 2A peptides on transgene expression mediated by tricistronic vectors in transfected CHO cells, Mol. Biol. Rep. 47 (2020) 469–475.
[30] P. Wongsodirdjo, A.C. Caruso, A.K. Yong, M.A. Lester, L.J. Vella, Y.H. Hung, R. M. Nisbet, Messenger RNA-encoded antibody approach for targeting extracellular and intracellular tau, Brain Commun. 6 (2024) fcae100.
[31] A.G. Orlandini von Niessen, M.A. Poleganov, C. Rechner, A. Plaschke, L.M. Kranz, S. Fesser, M. Diken, M. Lower, B. Vallazza, T. Beissert, V. Bukur, A.N. Kuhn, O. Tureci, U. Sahin, Improving mRNA-based therapeutic gene delivery by expression-augmenting 3' UTRs identified by cellular library screening, Mol. Ther. 27 (2019) 824–836.
[32] A. Kirshina, O. Vasileva, D. Kunyk, K. Seregina, A. Muslimov, R. Ivanov, V. Reshetnikov, Effects of combinations of untranslated-region sequences on translation of mRNA, Biomolecules 13 (2023).
[33] S. Linares-Fernandez, J. Moreno, E. Lambert, P. Mercier-Gouy, L. Vachez, B. Verrier, J.Y. Exposito, Combining an optimized mRNA template with a double purification process allows strong expression of in vitro transcribed mRNA, Mol. Ther. Nucleic Acids 26 (2021) 945–956.
[34] B. Li, X. Luo, Y. Dong, Effects of chemically modified messenger RNA on protein expression, Bioconjug. Chem. 27 (2016) 849–853.
[35] S. Vaidyanathan, K.T. Azizian, A. Haque, J.M. Henderson, A. Hendel, S. Shore, J. S. Antony, R.I. Hogrefe, M.S.D. Kormann, M.H. Porteus, A.P. McCaffrey, Uridine depletion and chemical modification increase Cas9 mRNA activity and reduce immunogenicity without HPLC purification, Mol. Ther. Nucleic Acids 12 (2018) 530–542.
[36] H. Moradian, T. Roch, L. Anthofer, A. Lendlein, M. Gossen, Chemical modification of uridine modulates mRNA-mediated proinflammatory and antiviral response in primary human macrophages, Mol. Ther. Nucleic Acids 27 (2022) 854–869.
[37] Y.V. Svitkin, Y.M. Cheng, T. Chakraborty, V. Presnyak, M. John, N. Sonenberg, N1-methyl-pseudouridine in mRNA enhances translation through eIF2alpha-dependent and independent mechanisms by increasing ribosome density, Nucleic Acids Res. 45 (2017) 6023–6036.
[38] Y.V. Svitkin, A.C. Gingras, N. Sonenberg, Membrane-dependent relief of translation elongation arrest on pseudouridine- and N1-methyl-pseudouridine-modified mRNAs, Nucleic Acids Res. 50 (2022) 7202–7215.
[39] H. Moradian, M. Schwestka, T. Roch, M. Gossen, Deconvolution of synthetic mRNA expression: nucleoside chemistry alters translatability, Bioeng. Transl. Med. 9 (2024) e10622.
[40] J.R. Melamed, K.A. Hajj, N. Chaudhary, D. Strelkova, M.L. Arral, N. Pardi, M. G. Alameh, J.B. Miller, L. Farbiak, D.J. Siegwart, D. Weissman, K.A. Whitehead, Lipid nanoparticle chemistry determines how nucleoside base modifications alter mRNA delivery, J. Control. Release 341 (2022) 206–214.
[41] B. Roy, Effects of mRNA modifications on translation: an overview, Methods Mol. Biol. 2298 (2021) 327–356.